北京航空航天大学
BEIHANG UNIVERSITY

Antenna Theory and Design

Associate Professor:
WANG Junjun 王珺珺

School of Electronic and Information Engineering, Beihang University

wangjunjun@buaa.edu.cn

13426405497

Chapter 6
Broadband Antennas

Chapter 6 Broadband Antennas

- Broadband Basics
- Helical Antennas
- Biconical Antennas
- Sleeve Antennas
- The Frequency-Independent Concept: Rumsey's Principle
- The Frequency-Independent Spiral Antennas
- The Log-periodic Antenna

6.1 Broadband Basics

- In many applications an antenna must operate effectively over a wide range of frequencies. An antenna with wide bandwidth is referred to as a broadband antenna.

- The bandwidth as a percent of the center frequency is (for narrow band antennas)

$$\frac{f_U - f_L}{f_C} \times 100 \qquad (6.1)$$

- Bandwidth is also defined as a ratio by (for wide band antennas)

$$\frac{f_U}{f_L} \qquad (6.2)$$

- The resonant antennas have small bandwidth.

- Antennas (e.g. Fig. 6.1 and 6.2) that have traveling waves on them rather than standing waves operate over wider frequency ranges.

- The definition of a broadband antenna is somewhat arbitrary and depends on the particular antenna. A working definition: If the impedance and the pattern of an antenna do not change significantly over an octave ($f_U/f_L = 2$) or more, we will classify it as a broadband antenna.

- Smooth physical structures(e.g. Fig. 6.1) tend to produce patterns and input impedances that also change smoothly with frequency. This simple concept is very prominent in broadband antennas.
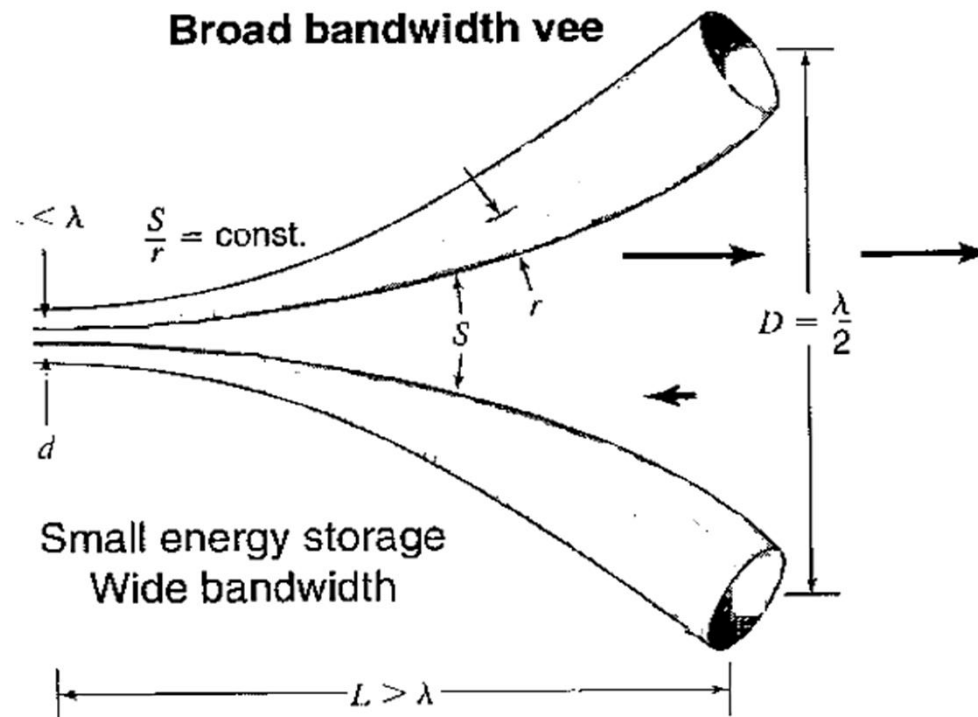
Broad bandwidth vee

$< \lambda$ $\frac{S}{r} = \text{const.}$

S r

$D = \frac{\lambda}{2}$

d

Small energy storage
Wide bandwidth

$L > \lambda$

Fig. 6.1 Broad bandwidth vee

6.2 Helical Antennas

Fig. 6.2 Several wideband helical antennas

6.2 Helical Antennas

- Another basic, simple, and practical configuration of an electromagnetic radiator is that of a conducting wire wound in the form of a screw thread forming a helix, as shown in Fig. 6.3.

- In most cases the helix is used with a ground plane. The ground plane can take different forms. One is for the ground to be flat, as shown in Fig. 6.4. Typically the diameter of the ground plane should be at least $3\lambda/4$. However, the ground plane can also be cupped in the form of a cylindrical cavity or in the form of a frustrum cavity. In addition, the helix is usually connected to the center conductor of a coaxial transmission line at the feed point with the outer conductor of the line attached to the ground plane.
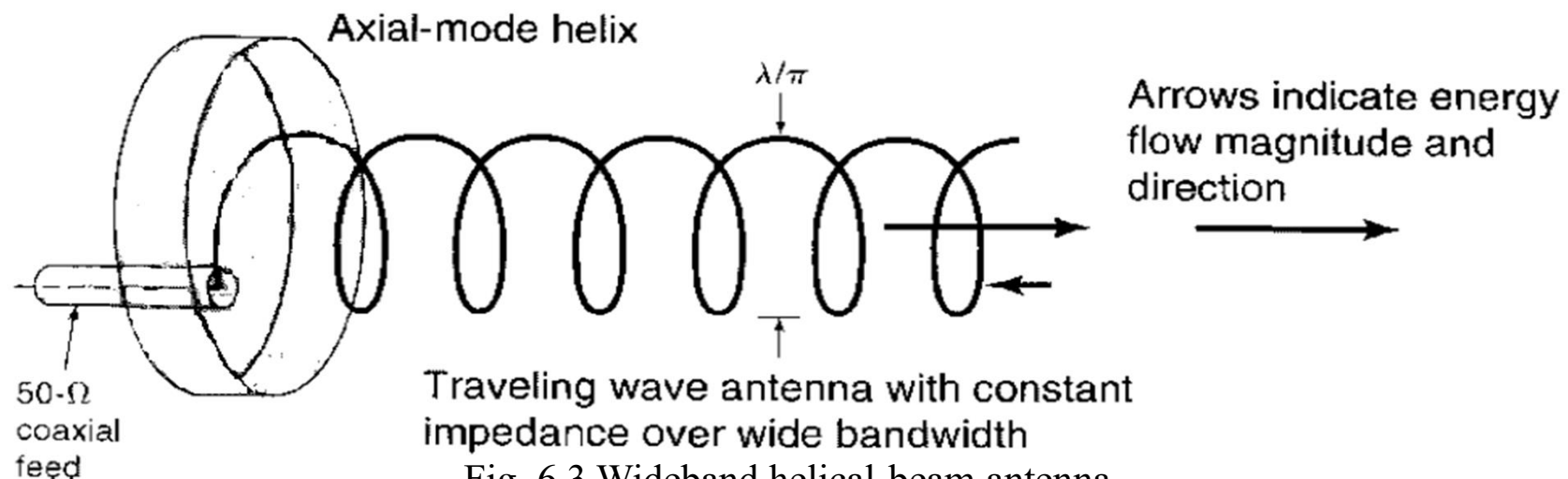

Fig. 6.3 Wideband helical-beam antenna

- If one turn of the helix is uncoiled the relationships among the various helix parameters are revealed.
- The symbols used to describe the helix are defined as follows:
- D = diameter of helix
  (between centers of coil material)
- C = circumference of helix = πD
- S = spacing between turns = $C \tan \alpha$
- α = pitch angle = $\tan^{-1} \dfrac{S}{C}$
- L_0 = length of turns
- L = axial length = NS
  (The geometrical configuration of a helix consists usually of N turns)
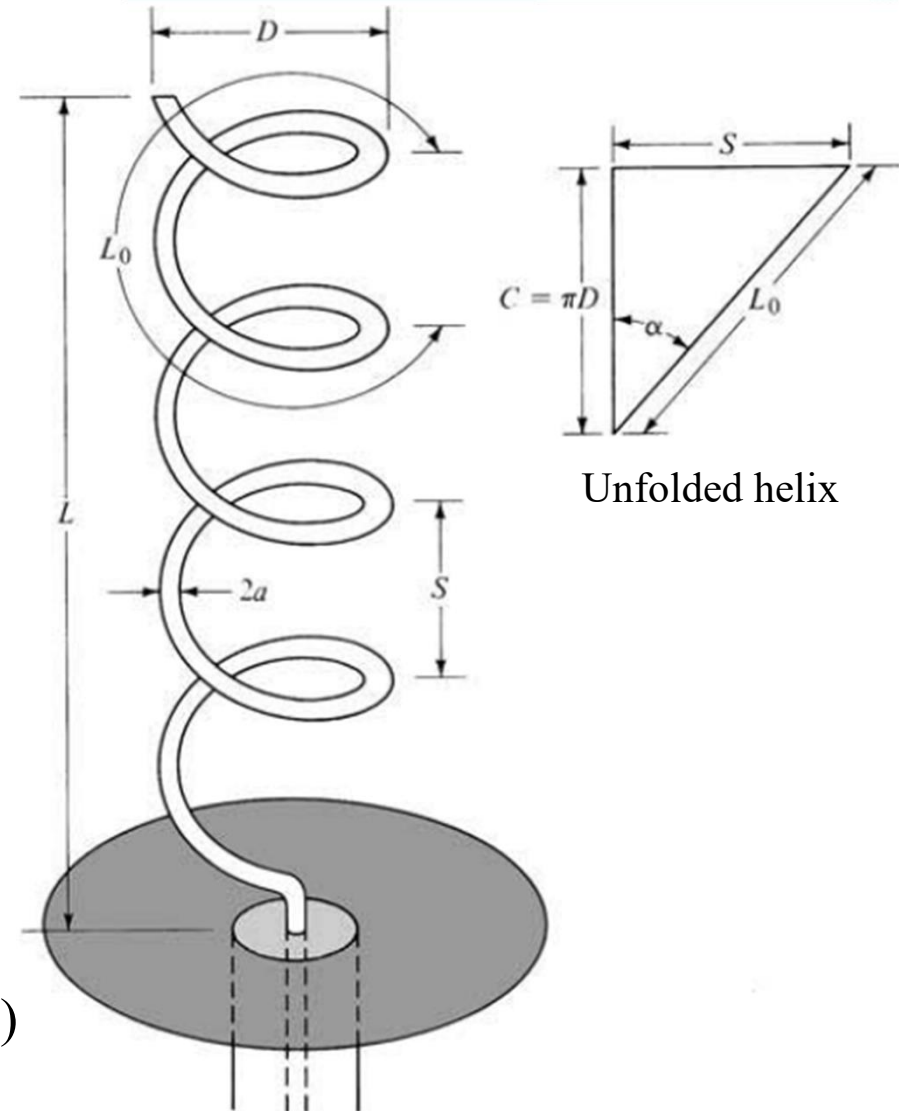- 2a = diameter of helix conductor

Unfolded helix

Fig. 6.4 Helical antenna with ground plane.

- Note that when $\alpha = 0°$, then the winding is flattened and the helix reduces to a loop antenna of N turns.

- On the other hand, when $\alpha = 90°$ then the helix reduces to a linear antenna. When $0° < \alpha < 90°$, then a true helix is formed with a circumference greater than zero but less than the circumference when the helix is reduced to a loop $(\alpha = 0°)$.

- The radiation characteristics of the antenna can be varied by controlling the size of its geometrical properties compared to the wavelength. The input impedance is critically dependent upon the pitch angle and the size of the conducting wire, especially near the feed point, and it can be adjusted by controlling their values. The general polarization of the antenna is elliptical. However circular and linear polarizations can be achieved over different frequency ranges.

- The helical antenna can operate in many modes; however the two principal ones are the *normal (broadside)* and the *axial (end-fire)* modes. The three-dimensional amplitude patterns representative of a helix operating, respectively, in the normal (broadside) and axial (end-fire) modes are shown in Fig. 6.5.
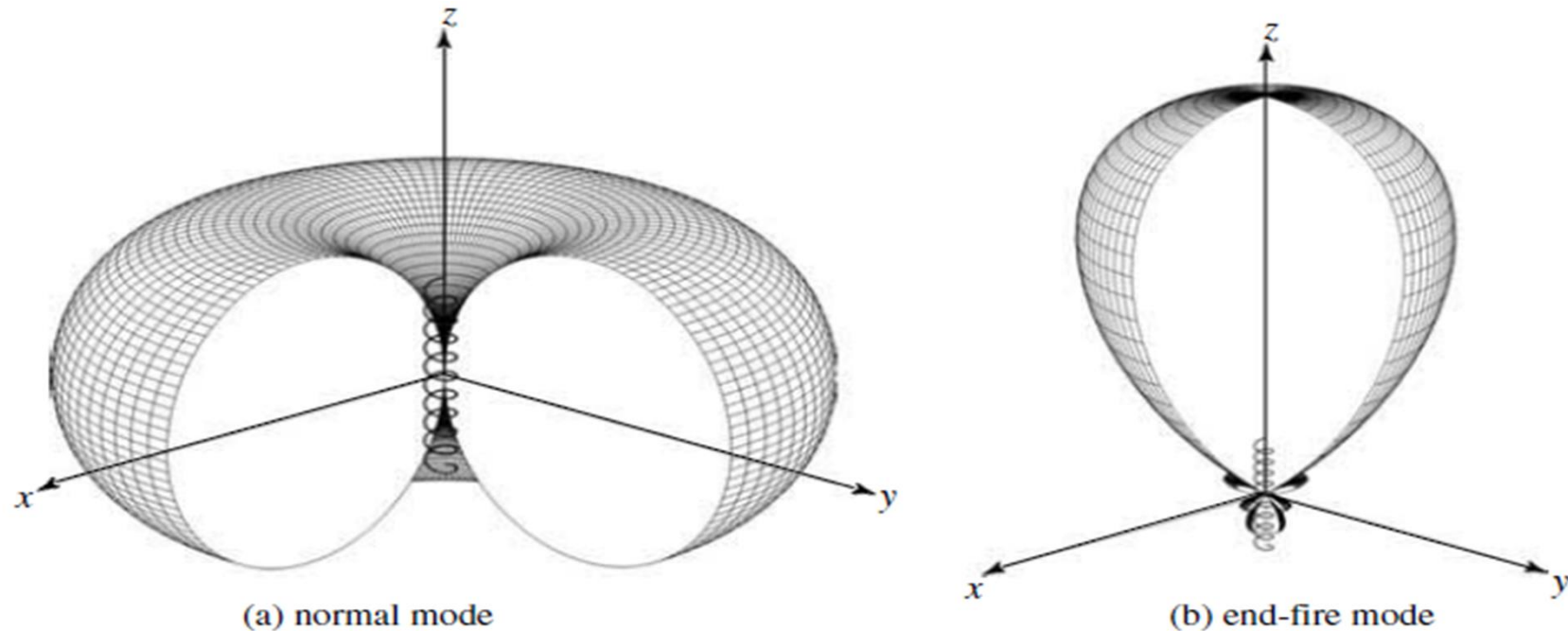

(a) normal mode　　　(b) end-fire mode

Figure 6.5 Three-dimensional normalized amplitude linear power patterns for *normal* and *end-fire* modes helical designs.
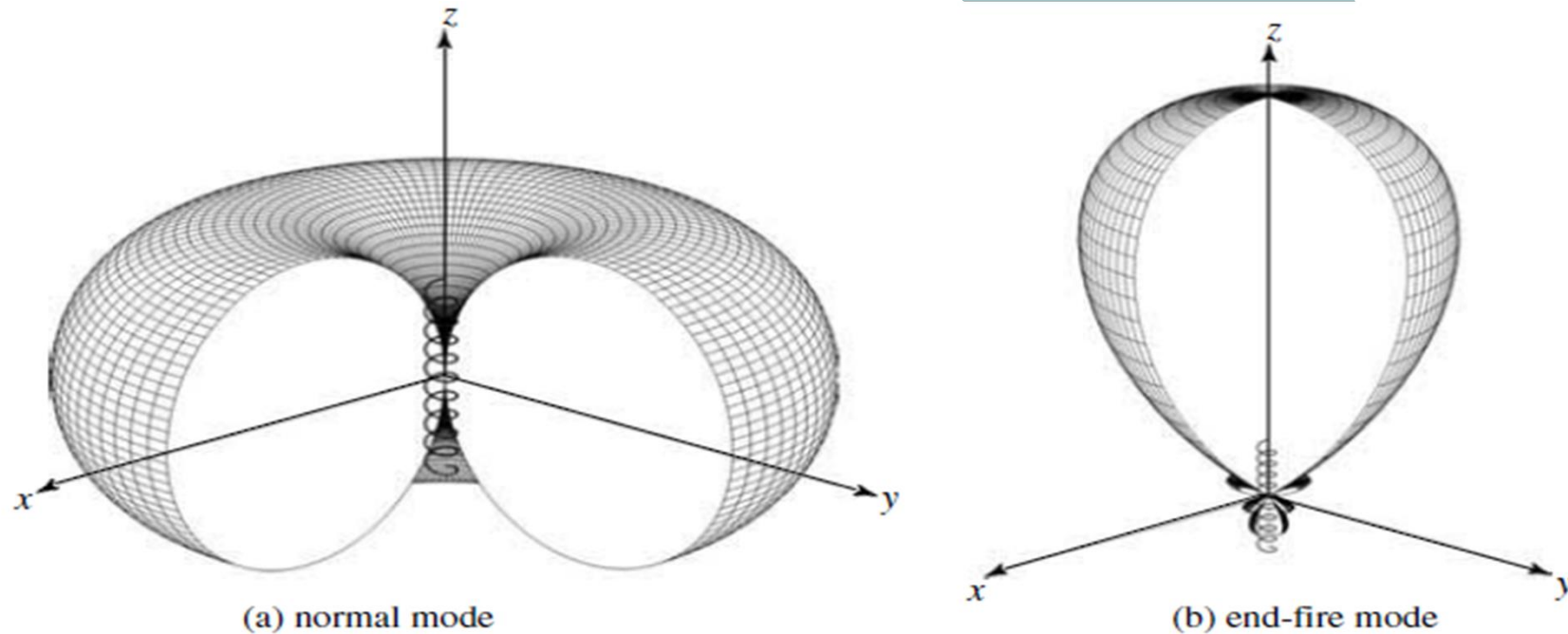
(a) normal mode

(b) end-fire mode

Figure 6.5 Three-dimensional normalized amplitude linear power patterns for *normal* and *end-fire* modes helical designs.

- **The normal mode**: yields radiation that is most intense normal to the axis of the helix. This occurs when the helix diameter is small compared to a wavelength.

- **The axial mode:** provides a radiation maximum along the axis of the helix. When the helix circumference is on the order of a wavelength the axial mode will result.

6.2.1 Normal Mode of Radiation

- For normal mode operation the dimensions of the helix must be small compared to a wavelength, i.e. $D \ll \lambda$. The normal mode helix is electrically small and thus its efficiency is low.
- Since the helix is small, the current is assumed to be constant in magnitude and phase over its length. The far-field pattern is independent of the number of turns and may be obtained by examining one turn. One turn can be approximated as a small loop and an ideal dipole as shown in Fig. 6.6.
- The far-zone electric field of the ideal dipole

$$E_D = j\omega\mu IS \frac{e^{-j\beta r}}{4\pi r} \sin\theta \, \hat{\theta} \qquad (6.3)$$

- The far-zone electric field of the small loop

$$E_L = \eta\beta^2 \frac{\pi}{4} D^2 \frac{e^{-j\beta r}}{4\pi r} \sin\theta \, \hat{\emptyset} \qquad (6.4)$$

- The total radiation field for one turn is the vector sum

$$E = E_D + E_L \qquad (6.5)$$

- The axial ratio of the polarization ellipse is found as

$$|AR| = \left|\frac{E_\theta}{E_\phi}\right| = \frac{2S\lambda}{\pi^2 D^2} \qquad (6.6)$$
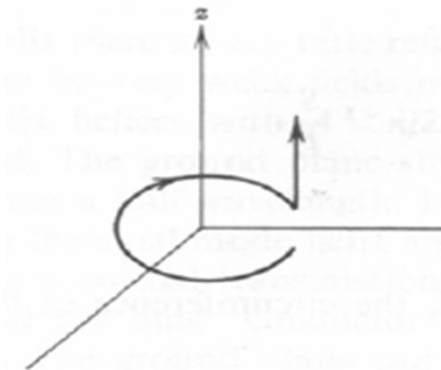
Fig. 6.6 One turn of a normal mode helix approximated as a small loop and an ideal dipole.

Since the perpendicular linear components are 90° out-of-phase, circular polarization is obtained if the axial ratio is unity. This occurs for

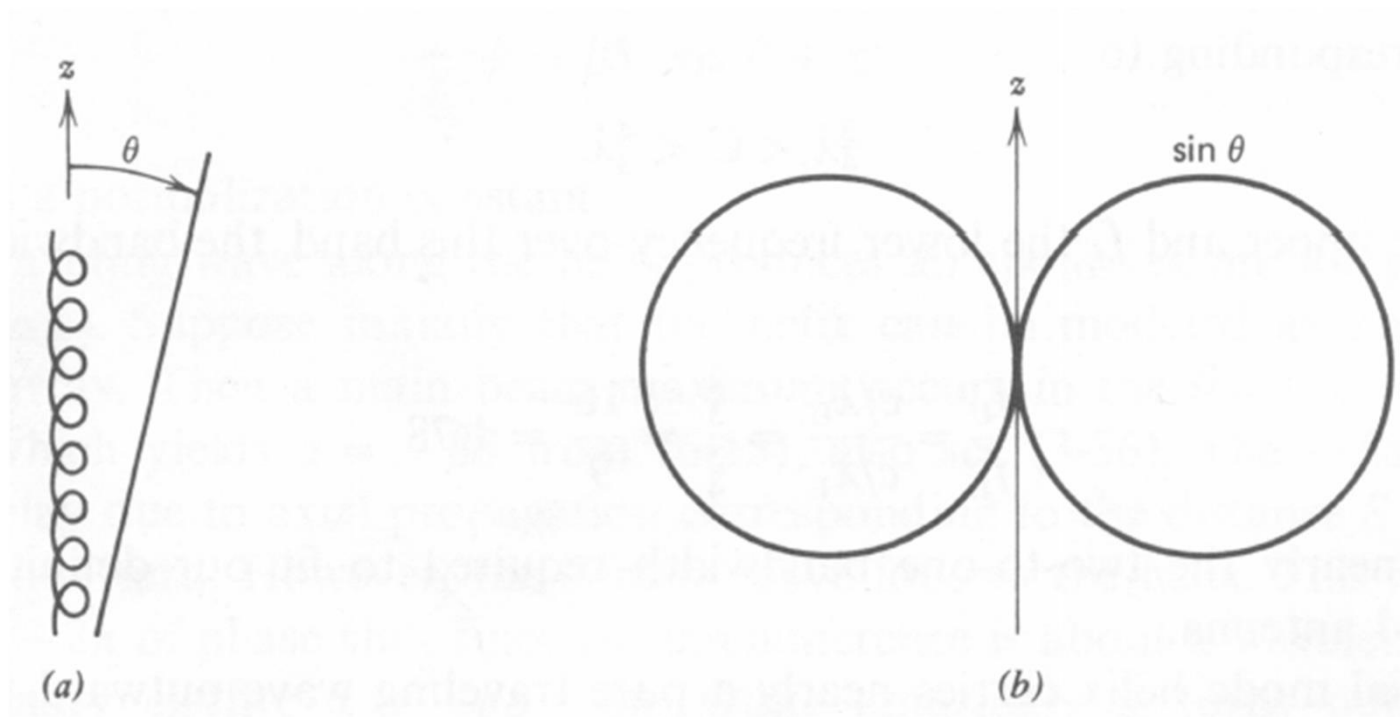$$\pi D = \sqrt{2S\lambda} \qquad (6.7)$$

Fig. 6.7 The normal mode helix (a) and its radiation pattern (b).

To achieve the normal mode of operation, it has been assumed that the current throughout the helix is of constant magnitude and phase. This is satisfied to a large extent provided the total length of the helix wire NL_0 is very small compared to the wavelength $(L_n \ll \lambda_0)$ and its end is terminated properly to reduce multiple reflections. Because of the critical dependence of its radiation characteristics on its geometrical dimensions, which must be very small compared to the wavelength, this mode of operation is very narrow in bandwidth and its radiation efficiency is very small. Practically this mode of operation is limited, and it is seldom utilized.
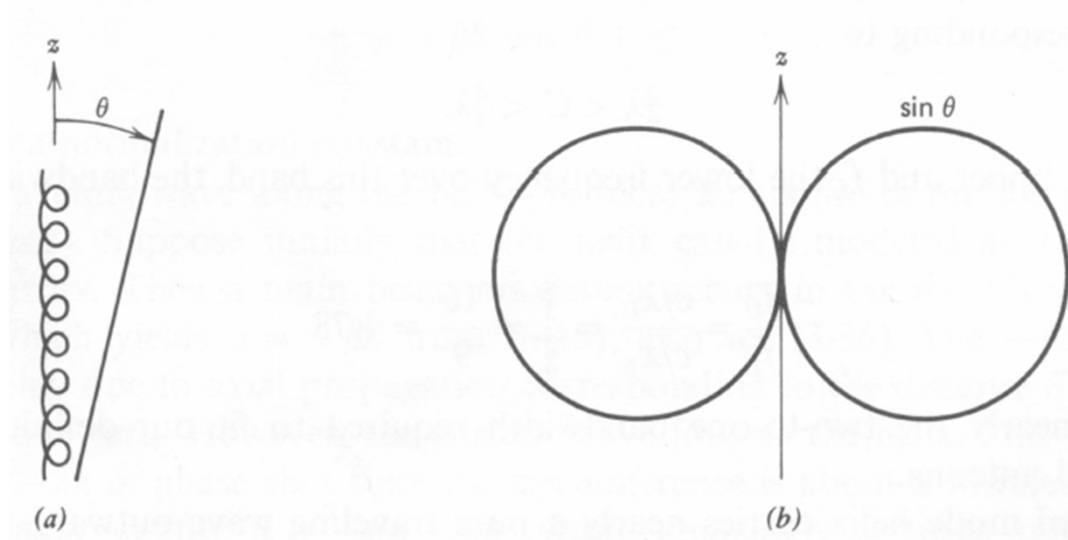

Fig. 6.7 The normal mode helix (a) and its radiation pattern (b).

6.2.2 Axial Mode of Radiation

In the axial mode of radiation the helix radiates as an end-fire antenna with a single maximum along the axis of the helix.

- The radiation is close to circular polarization near the axis.
- The half-power beamwidth can be reduced by increasing the number of turns.
- The axial mode occurs when the helix circumference is on the order of a wavelength.
- In fact, the expression presented in this section remain valid over at least a frequency range corresponding to

$$\frac{3}{4}\lambda < C < \frac{4}{3}\lambda \tag{6.8}$$

- The bandwith ratio

$$\frac{f_U}{f_L} = \frac{c/\lambda_U}{c/\lambda_L} = \frac{\frac{4}{3}}{\frac{3}{4}} = 1.78 \tag{6.9}$$

- The axial mode helix carries nearly a pure traveling wave outward from the feed.

The current at opposite points of a turn is essentially in phase, leading to far-field reinforcement along the helix axis. The radiation pattern can be found by considering the helix to be an array of N identical elements (or turns).

- The element pattern for one turn is approximately that of a one-wavelength loop. An approximation for is $\cos\theta$.
- Assuming equal amplitude of excitation for each turn, the array factor is that of a uniformly excited, equally spaced array.

The total pattern is then

$$F(\theta) = K\cos(\theta)\frac{\sin(N\psi/2)}{N\sin(\psi/2)} \qquad (6.10)$$

Where $\psi = \beta S\cos\theta + \alpha$.

- Suppose initially that the helix can be modeled as an ordinary end-fire array. Then a main beam maximum occurs in the $\theta = 0°$ direction for $\psi = 0°$, which yields $\alpha = -\beta S$. The $-\beta S$ phase is phase delay due to axial propagation corresponding to the distance S along the axis for one turn. However, the current wave follows the helix. This introduce another -2π of phase shift since the circumference is about a wavelength. Thus for ordinary end-fire $\alpha = -\beta S - 2\pi$. Quite amazingly it turns out that the traveling-wave mode on the axial mode helix corresponds to nearly a naturally occurring Hansen Woodyard increased directivity type end-fire array.

- Thus, the element-to-element phase shift is

$$\alpha = -\left(\beta S + 2\pi + \frac{\pi}{N}\right) \tag{6.11}$$

- This phase shift leads to a value for the phase velocity of the traveling wave. Let β_h be the phase constant associated with wave propagation along the helical conductor, then we have

$$\alpha = -\left(\beta S + 2\pi + \frac{\pi}{N}\right) = -\beta_h L \tag{6.12}$$

$$\beta_h = \frac{1}{L}\left(\beta S + 2\pi + \frac{\pi}{N}\right) \tag{6.13}$$

- The velocity factor(phase velocity relative to the free-space velocity of light) is

$$p = \frac{v}{c} = \frac{\omega/c}{\omega/v} = \frac{\beta}{\beta_h} = \frac{L/\lambda}{S/\lambda + (2N+1)/2N} \qquad (6.14)$$

For a typical configuration:

- $C = \lambda, \alpha = 12°$ and $N = 12$, then $S = C \tan \alpha = 0.213\lambda$, $L = \sqrt{C^2 + S^2} = 1.022\lambda$, and $p = 0.815$. Therefore, the traveling wave has a phase velocity less than that if it were a plane wave in free space. Such a wave is referred to as a slow wave. Another remarkable feature of the helix is that as the helix parameter vary over rather large ranges ($5° < \alpha < 20°$ and $\frac{3}{4}\lambda < C < \frac{4}{3}\lambda$)the phase velocity adjusts automatically to maintain increased directivity.

- In general, end-fire mode is a more practical mode of operation, and the terminal impedance of a helical antenna operating in the axial mode is nearly purely resistive since it is essentially a traveling-wave antenna. An empirically derived formula for input resistance is $R_{in} = 140 \frac{C}{\lambda} \Omega$.

- Most often the antenna is used in conjunction with a ground plane, whose diameter is at leas $\lambda_0/2$, and it is fed by a coaxial line. However other types of feeds (such as waveguides an dielectric rods) are possible, especially at microwave frequencies. The dimensions of the helix for this mode of operation are not as critical, thus resulting in a greater bandwid
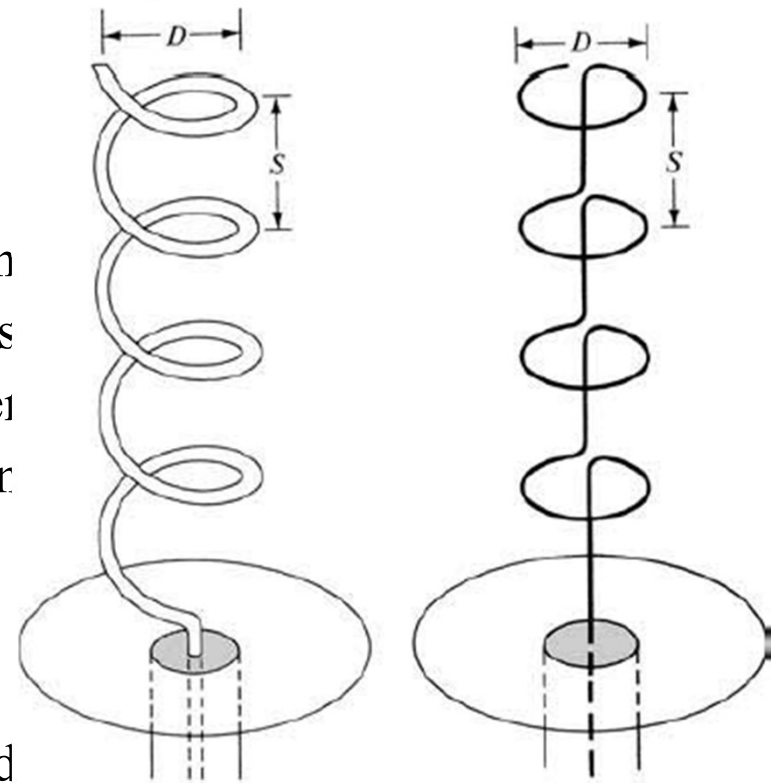

Fig. 6.8 Mode for helical antenna and its equivalent

6.3 Biconical Antennas

The bandwidth of a simple dipole antenna can be increased by using thicker wire. This concept can be extended to further increase bandwidth if the conductors are flared to form a biconical structure.

Fig. 6.9 Several wideband biconical antennas

6.3.1 The Infinite Biconical Antenna

An infinite biconical antenna acts as guide for a traveling outgoing spherical wave in the same way that a uniform transmission line acts as a guide for a traveling plane wave.
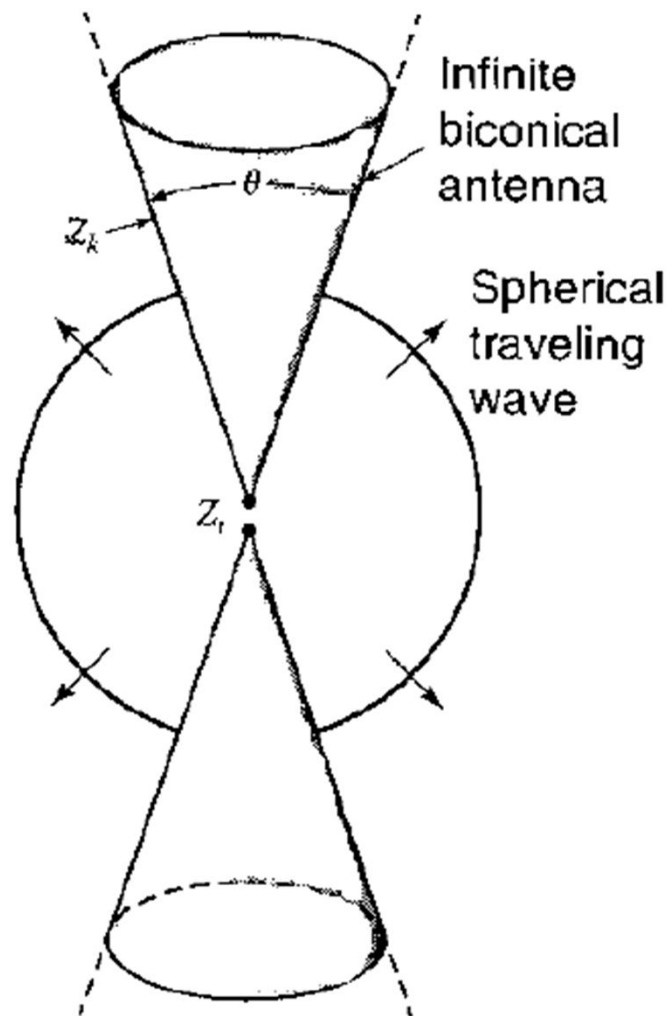
- The two situation are compared in Fig. 6.10. They both have a constant characteristic impedance Z_k and since they are infinite the input impedance $Z_i = Z_k$. These values are purely resistive so the input resistance
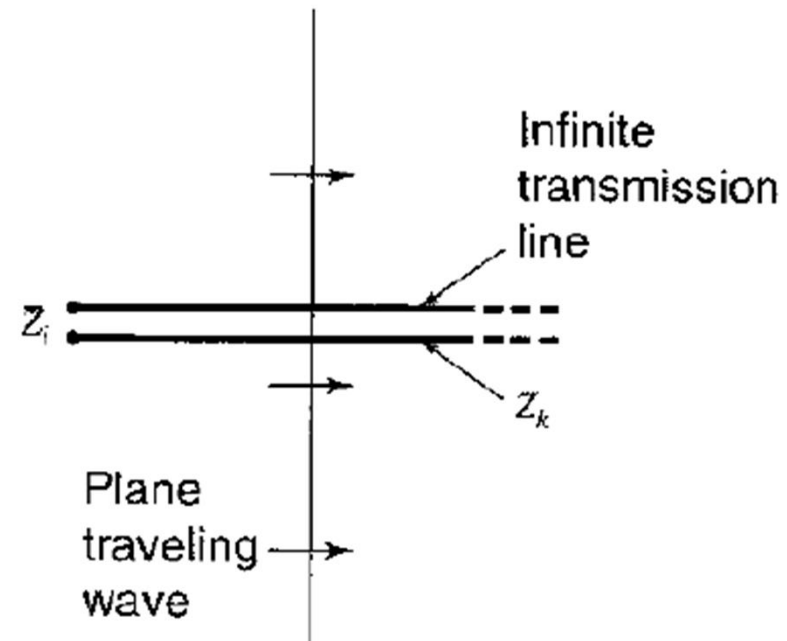
$$R_i = Z_i = Z_k \qquad (6.15)$$

- For the infinite biconical antenna

$$R_i = 120 \ln \cot(\theta/4) \qquad (6.16)$$

- Where $\theta = cone\ angle$

(a)   (b)

Fig. 6.10
An infinite biconical antenna(a) is analogous to an infinite uniform transmission line (b).

6.3.2 The Finite Biconical Antenna

- With the infinite biconical antenna as an introduction, let us now consider the practical case of a biconical antenna of finite radius r (Fig. 6.11). The ends of the cones cause reflections that set up standing waves that lead to a complex input impedance. The values of input impedance are plotted. When the outgoing spherical wave reaches a radius r part of the energy is reflected, resulting in energy storage. The remaining energy is radiated, with more radiated perpendicular to the axis than close to the cones as suggested in Fig. 6.11.
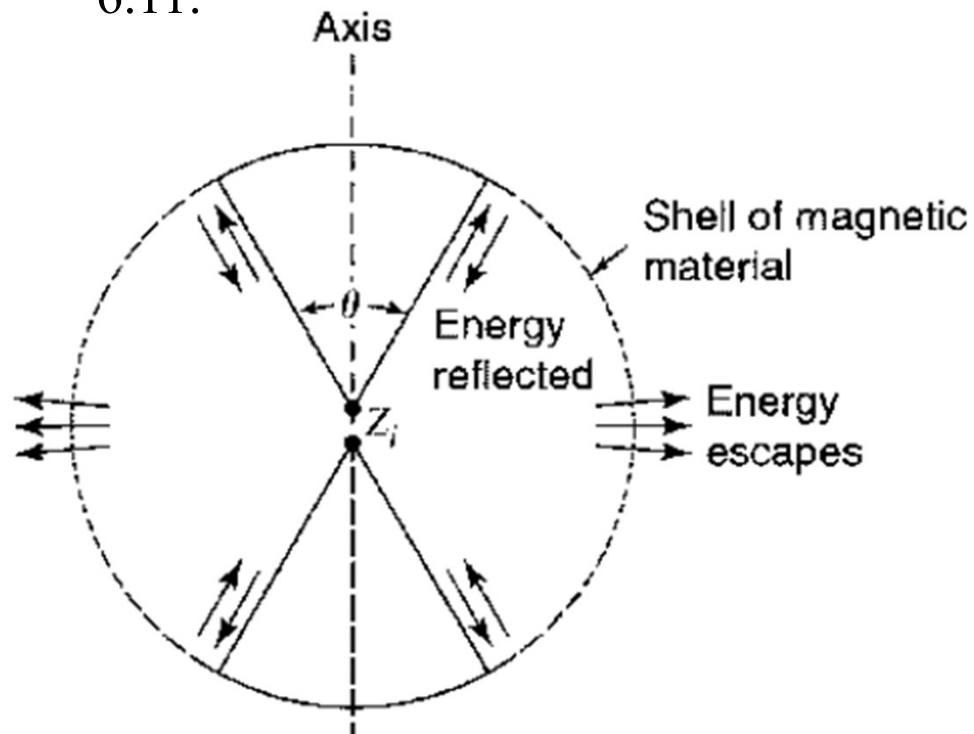

Fig. 6.11 Finite biconical antenna enclosed in hypothetical sphere where energy flowing near the cone is reflected but with energy escaping perpendicular to the axis in the equatorial region.

6.3.3 Directional Biconicals, Conicals, Disk Cones And Bow Ties

Fig. 6.12 shows a progression of V-type antennas from the simple V at (a) to the biconical V at (b) to the curved biconical V at (c). The characteristic impedance Z_k of the simple V at (a) is not constant and the V has a narrow bandwidth. Its pattern is bidirectional.

The biconical V at (b) has a constant characteristic impedance Z_k and the antenna has a wider bandwith. It also tends to be unidirectional.

The curved biconical antenna (c) also has a constant characteristic impedance Z_k, is more unidirectional and has a still wider bandwidth.
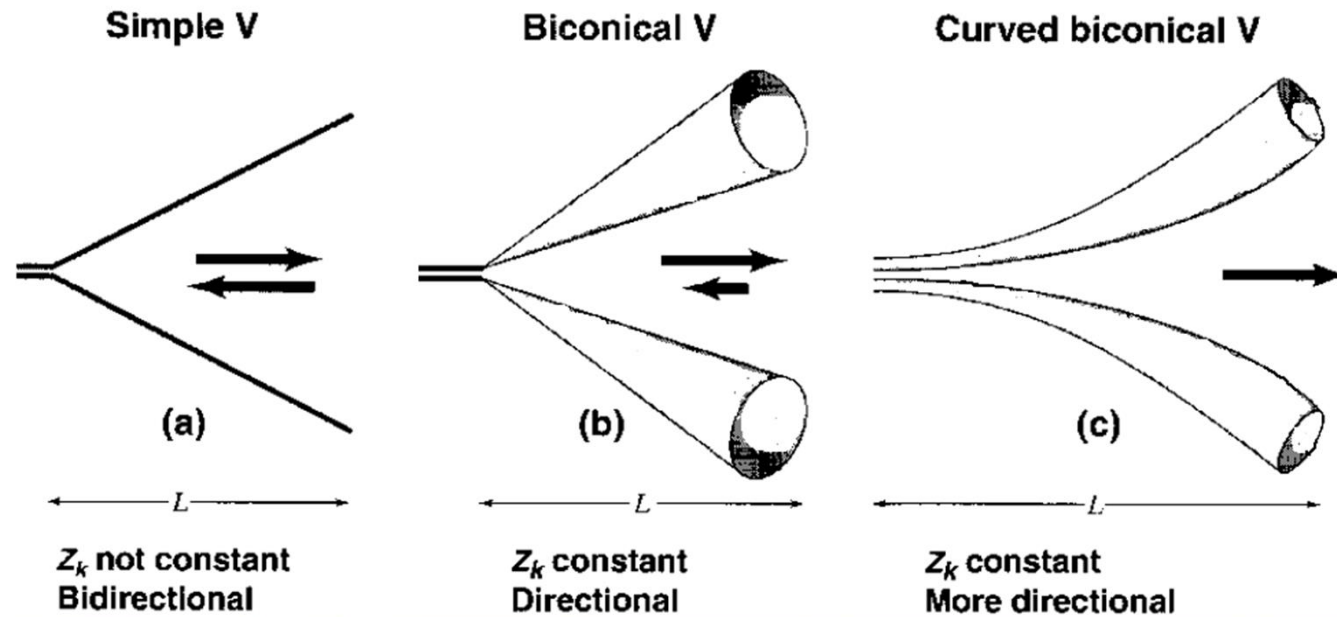

Fig. 6.12 (a)Simple V, (b) biconical V and (c) curved biconical V antennas having increasing bandwidth

Curved biconical V

(a)

Virtual resistances

Energy radiated

λ

Uniform line

(b) << λ
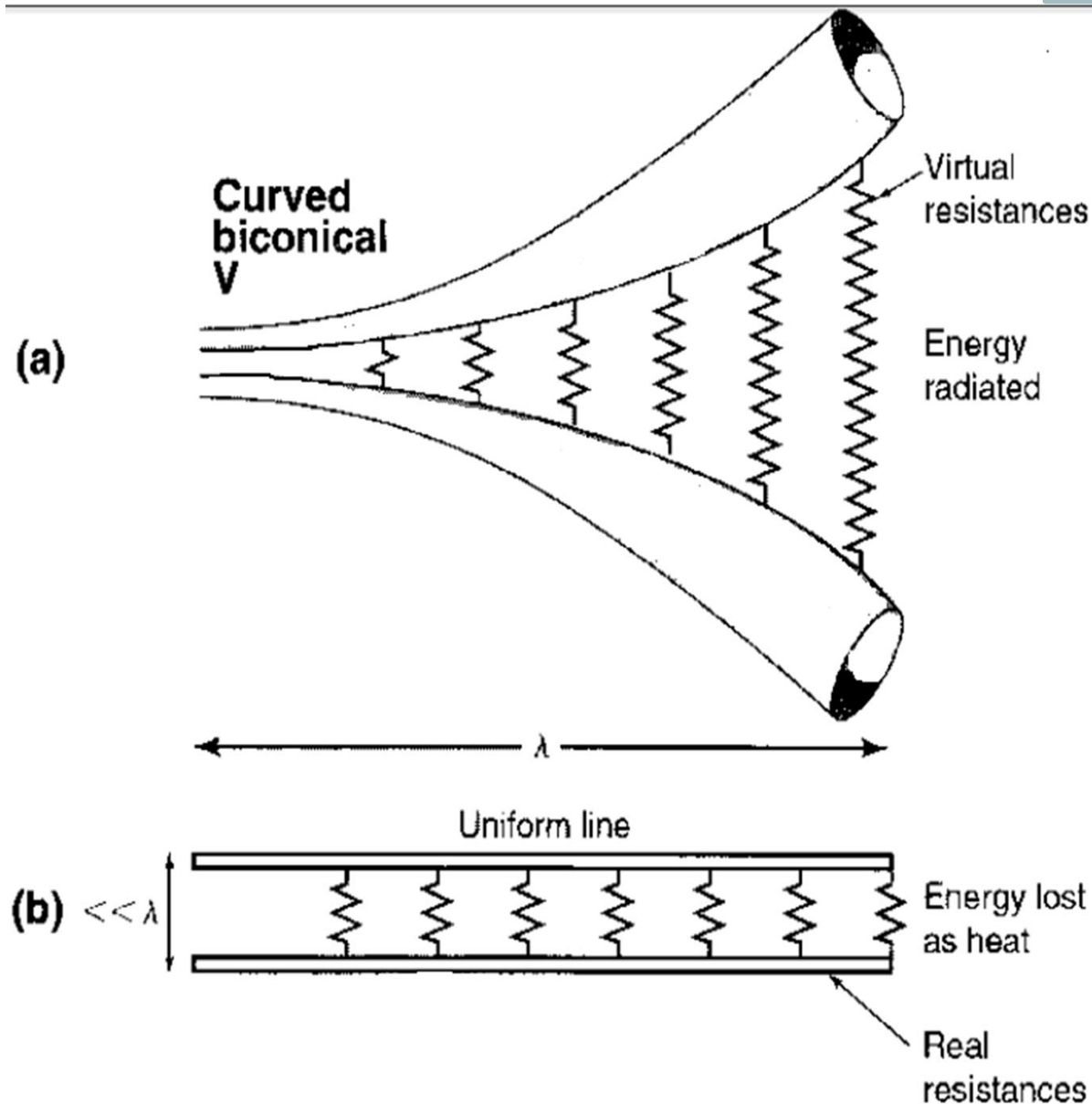
Energy lost as heat

Real resistances

Fig. 6.13

Comparison of curved biconical V antenna with a resistance-loaded uniform transmission line. Both have similar current distributions, decreasing from left to right. The virtual resistances of the biconical antenna radiate energy whereas the real resistances of the uniform line absorb energy which is lost as heat.

Fig. 6.14 shows a progression of conical antennas with coax feed. The one at (a) is a full biconical. The one at (b) has the upper cone replaced by a thin stub, while at (c) the cone is replaced by a disk. The coax feed makes these antennas convenient for mounting on masts. Radiation is a maximum in the horizontal plane.
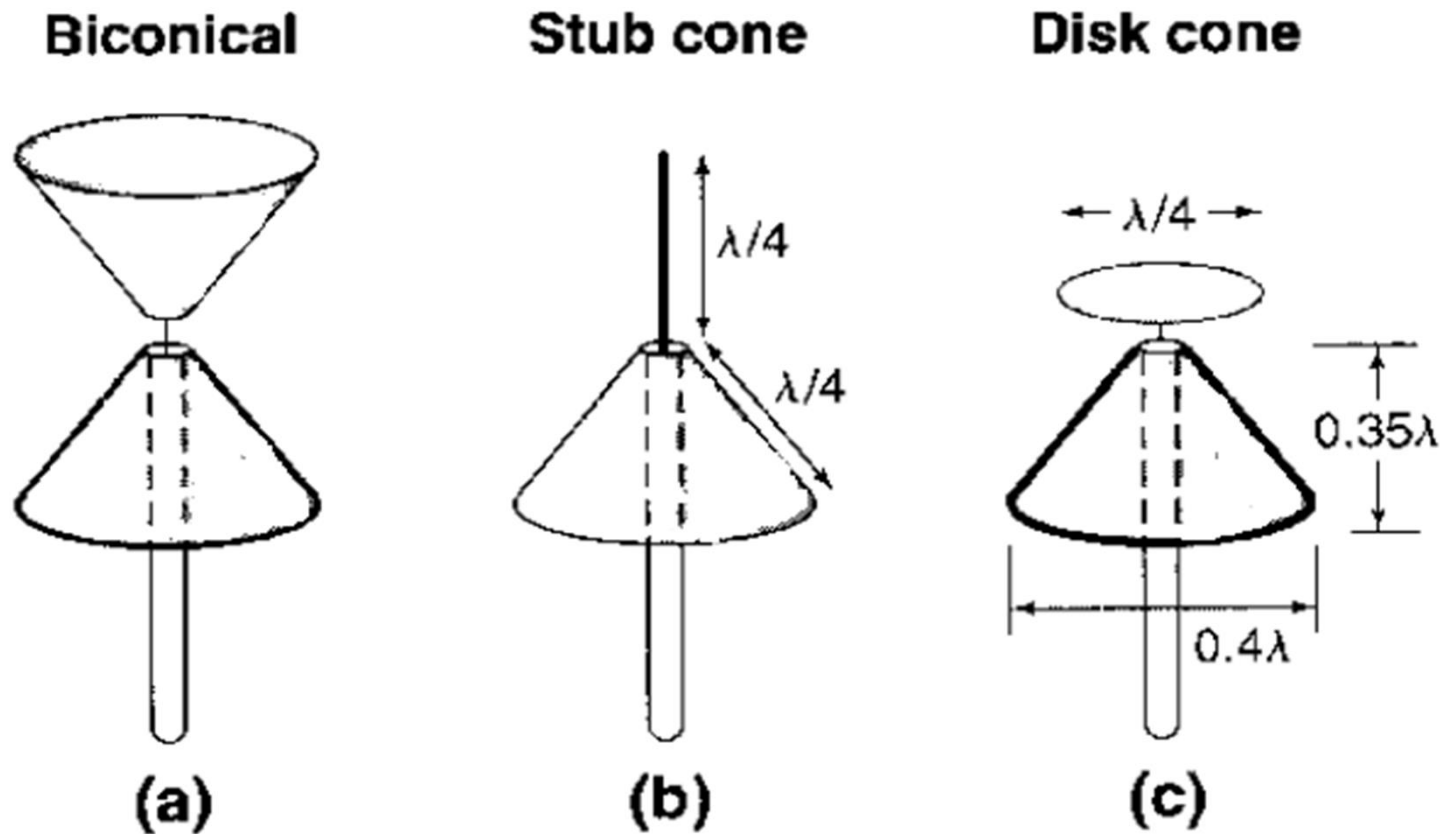
Biconical　　　　**Stub cone**　　　　**Disk cone**

(a)　　　　　(b)　　　　　(c)

Fig. 6.14 Coaxial fed conical antennas for mounting on masts whith omnidirectional radiation in the horizontal plane.

A bow-tie antenna(Brown(1) and Woodward) is a flat-plane version of the biconical antenna. The 60° bow tie of Fig. 6.15-a provides a VSRW< 2 over a 2 to 1 handwidth for $L = 0.8\lambda$ at the center frequency. An open-wire version of the biconical antenna is shown in Fig. 6.15-b with properties nearly the same as with solid surface cones.
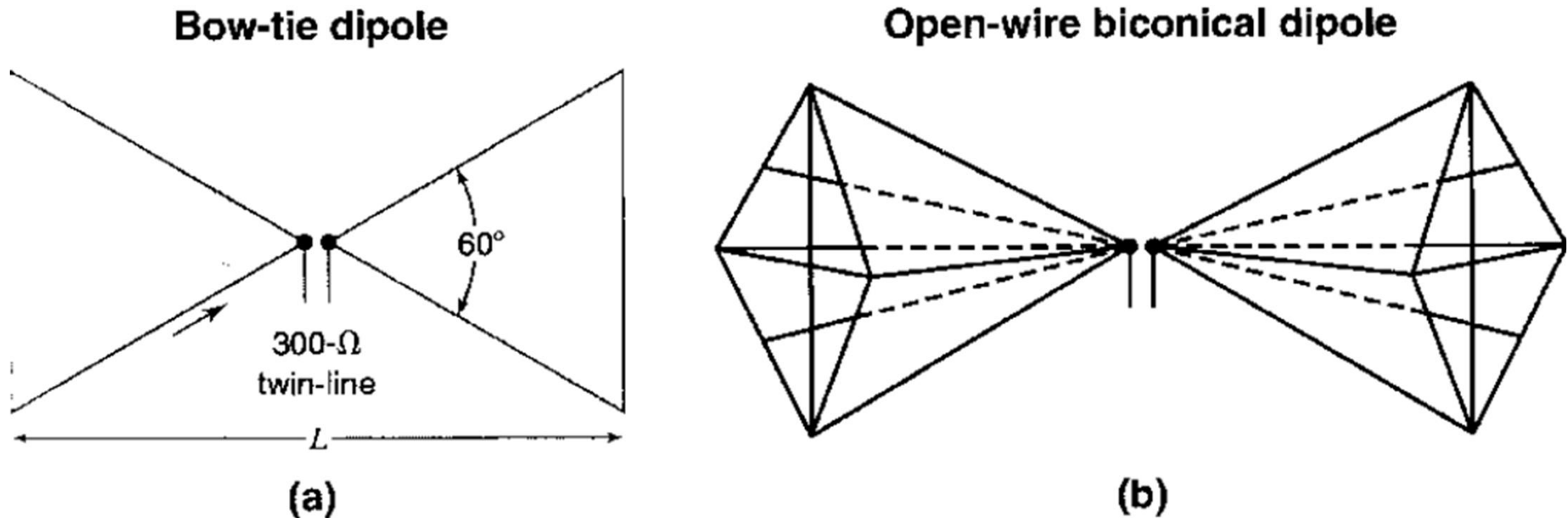
Bow-tie dipole

Open-wire biconical dipole

Fig. 6.15 (a)Flat-plane bow-tie antenna   (b) open-wire biconical dipole antenna

6.4 Sleeve Antennas

- The dipole antenna is very frequency sensitive and its bandwidth is much less than the octave bandwidth. The addition of a sleeve to a dipole or monopole can increase the bandwidth to more than an octave.

Fig. 6.16 Several wideband sleeve antennas

6.4.1 Sleeve Monopoles

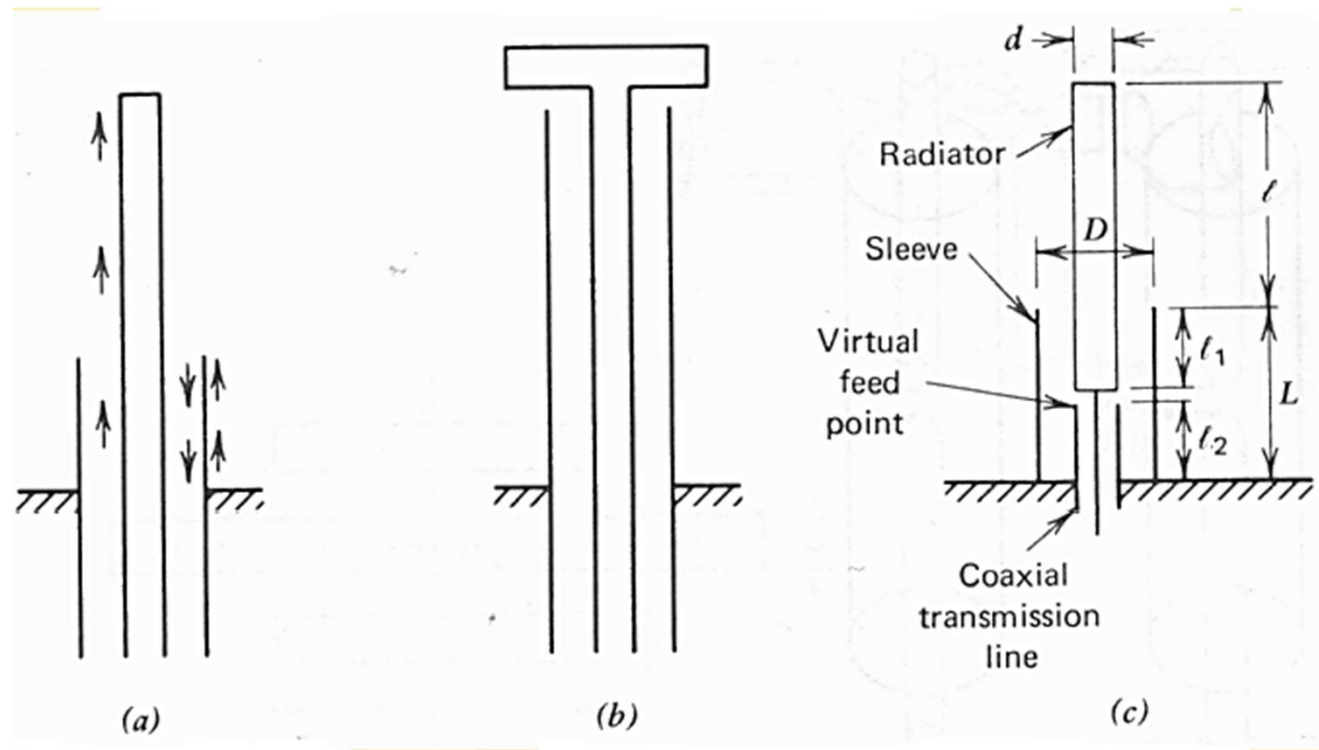Three sleeve monopole configurations are show in Fig.6.17. Fed from a coaxial transmission line.

Fig. 6.17 Sleeve monopole configurations
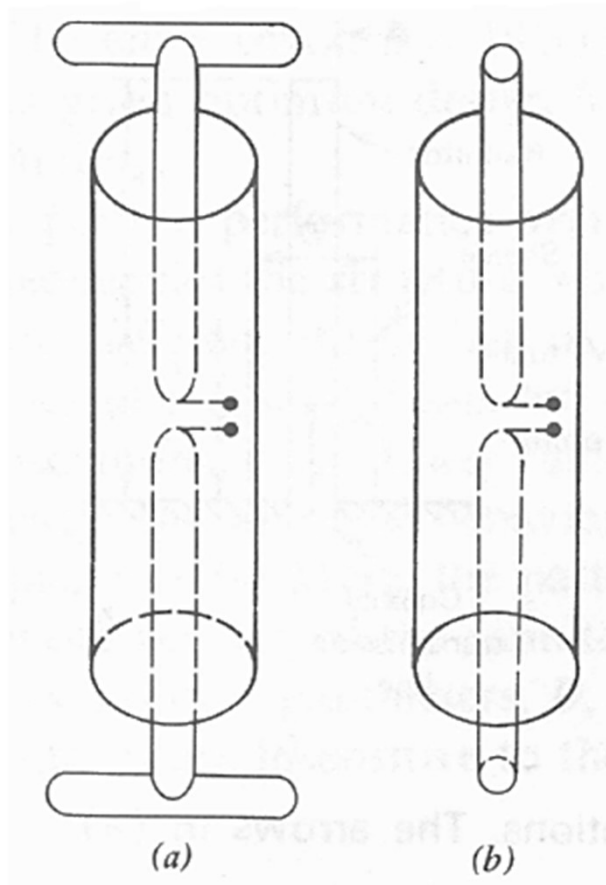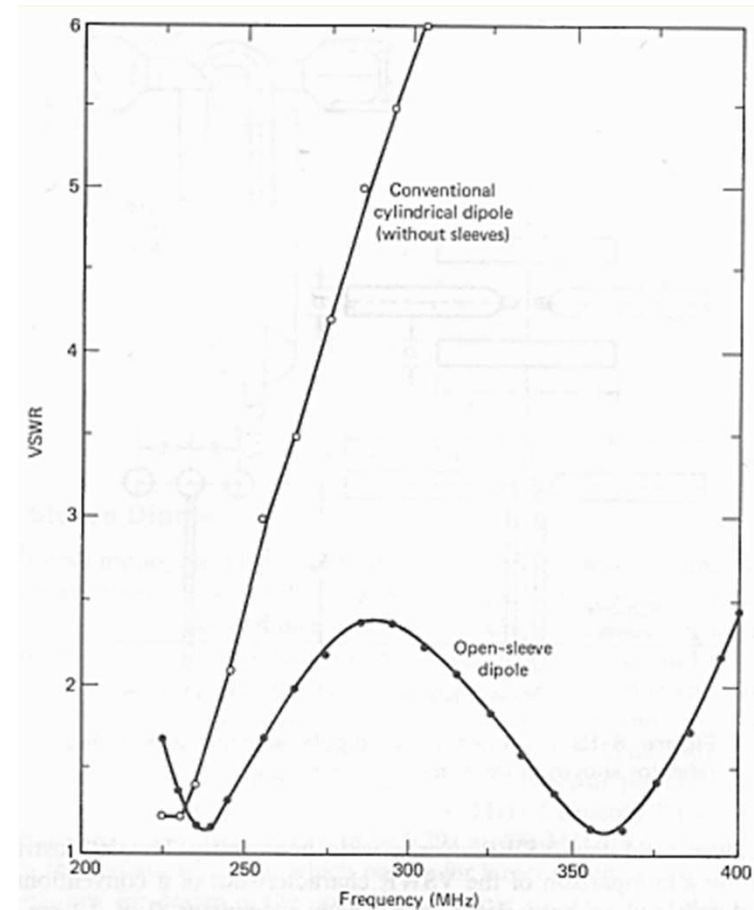
6.4.2 Sleeve Dipoles

Fig. 6.18 Sleeve dipole

Fig. 6.19 Comparison between the VSWR response of a conventional (unsleeved) cylindrical dipole both with a diameter of 2.9mm

6.5 The Frequency-Independent Concept: Rumsey's Principle

A true frequency-independent antenna is physically fixed in size and operates on an instantaneous basis over a wide bandwidth with relatively constant impedance, pattern, polarization and gain.

Rumsey's principle is that the impedance and pattern properties of an antenna will be frequency-independent if the antenna shape is specified only in terms of angles.

Thus , an infinite logarithmic spiral should meet the requirement. When truncated (without a matched termination) there is a reflected wave from the ends of the cones which results in modified impedance and pattern characteristics.

6.5.1 Rumsey's general equation

To meet the frequency-independent requirement in a finite structure requires that the current attenuate along the structure and be negligible at the point of truncation. For radiation and attenuation to occur, charge must be accelerated (or decelerated) and this happens when a conductor is curved or bent normally to the direction in which the charge is traveling. Thus, the curvature of a spiral results in radiation and attenuation so that, even when truncated ,the spiral provides frequency-independent operation over a wide bandwidth.

The surface of the antenna or surface edges have curve (as follows)to describe

$$r = F\ (\theta\ ,\ \varphi) =\ e^{\alpha\varphi}f\ (\theta)$$

$f\ (\theta)$ is an arbitrary function, thus the impedance and pattern properties of an antenna will be frequency-independent .

6.6 The Frequency-Independent Spiral Antennas

- The equation for a log-spiral is given by

$$r = a^\theta \qquad or \qquad \theta \ln a \qquad\qquad (6.17)$$

Where, referring to Fig. 6.20,

- r= radial distance to point P on spiral
- θ= angle with respect to x axis
- a= a constant

From (6.17), the rate of change go radius with angle is

$$\frac{dr}{d\theta} = a^\theta \ln a = r \ln a \qquad (6.18)$$

The constant a in (6.18) is related to the angle β between the spiral and a radial line from the origin as given by

$$\ln a = \frac{dr}{rd\theta} = \frac{1}{\tan \beta} \qquad (6.19)$$

Thus, from (6.19) and (6.17)

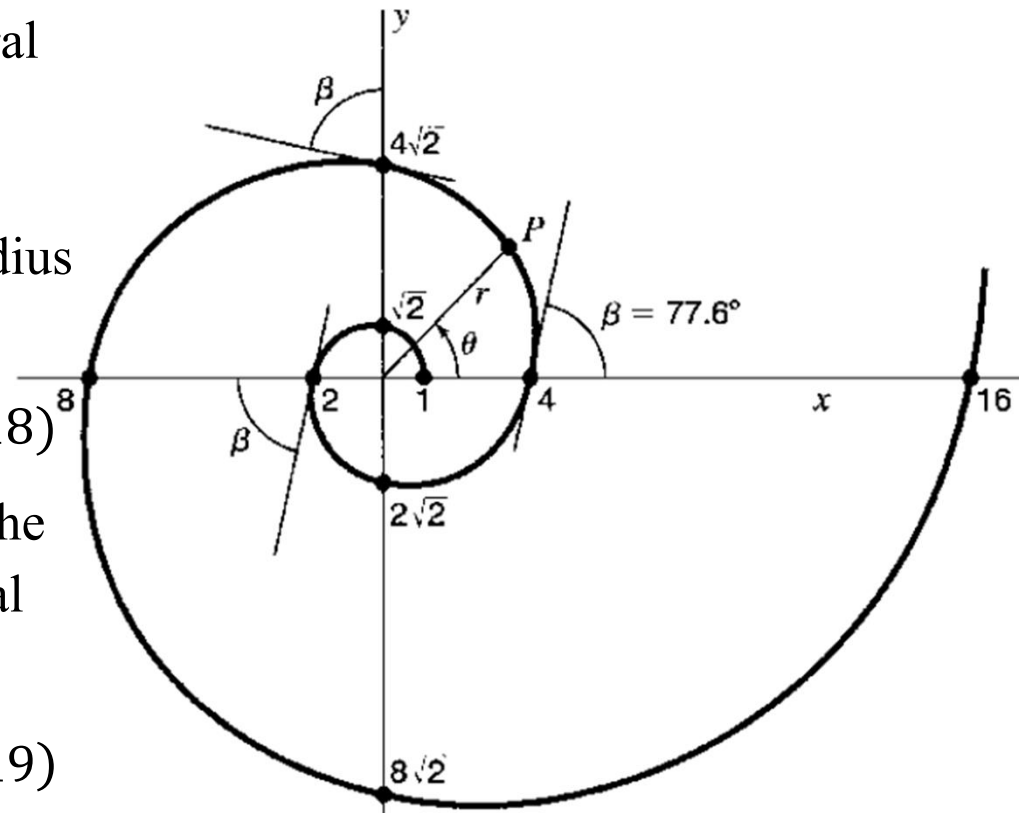$$\theta = \tan \beta \ln r \qquad\qquad (6.20)$$

Fig. 6.20 Log-spiral

6.6.1 The Frequency-Independent Planar Log-Spiral Antenna

Fig. 6.21 Several frequency-independent planar spiral antennas

6.6.1 The Frequency-Independent Planar Log-Spiral Antenna

For a rotation $\delta = \pi/2$ we have 4 spirals at 90° angles. Metalizing the areas between spirals 1 and 4 and 2 and 3, with the other areas open, self-complementary and congruence conditions are satisfied. Connecting a generator or receiver across the inner terminals, we obtain Dyson's frequency-independent planar spiral antenna of Fig. 6.22 .
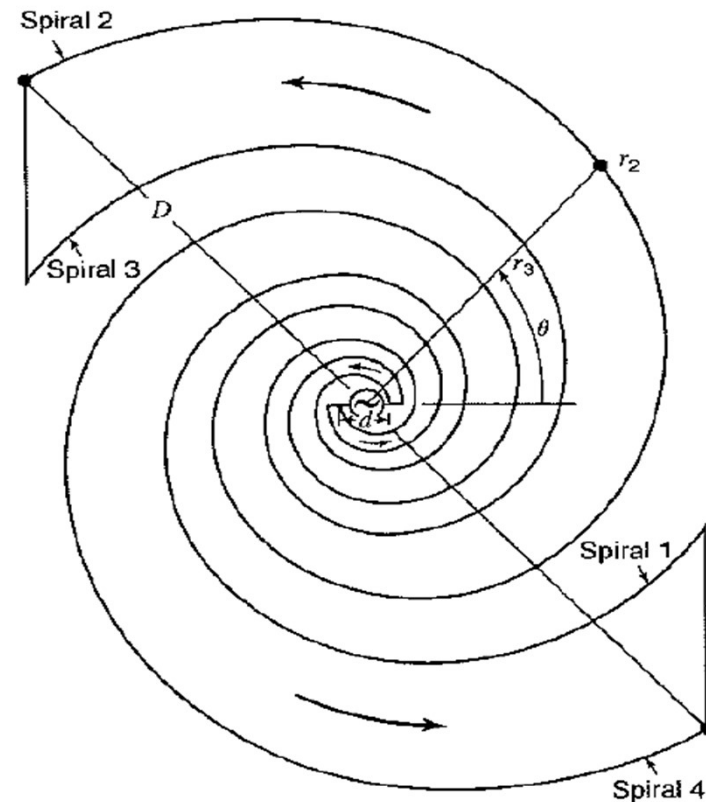
Fig. 6.22 Frequency-independent planar spiral antenna

6.6.1 The Frequency-Independent Planar Log-Spiral Antenna

The arrows indicate the direction of the outgoing waves traveling along the conductors resulting in right-circularly polarized radiation outward from the page and left-circularly polarized radiation into the page. The high-frequency limit of operation is determined by the spacing d of the input terminal and the low-frequency limit by the overall diameter D. The ratio D/d for the antenna of Fig. 6.18 is about 25 to 1. If we take $d = \lambda/10$ at the high-frequency limit and $D = \lambda/2$ at the low-frequency limit, the antenna bandwidth is 5 to 1.
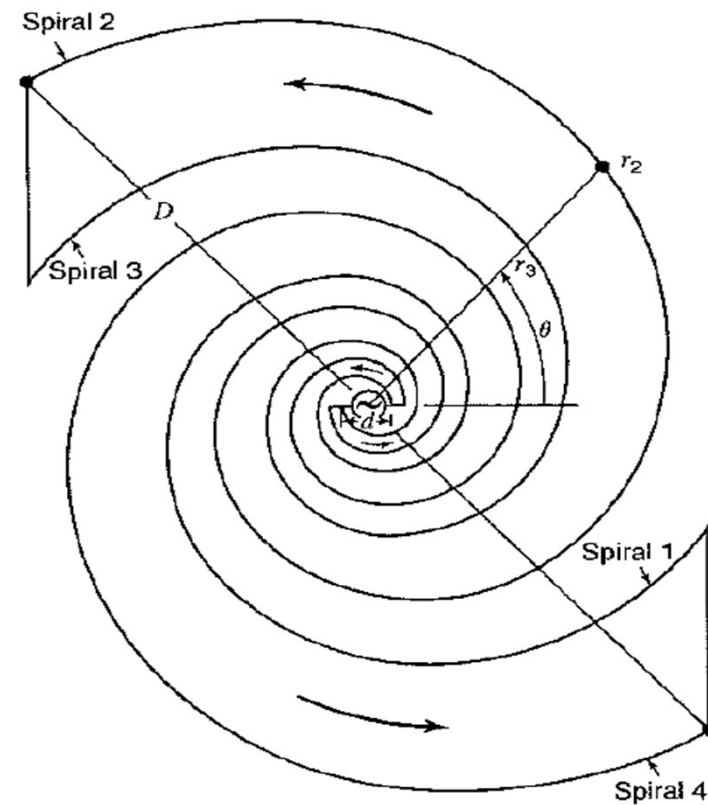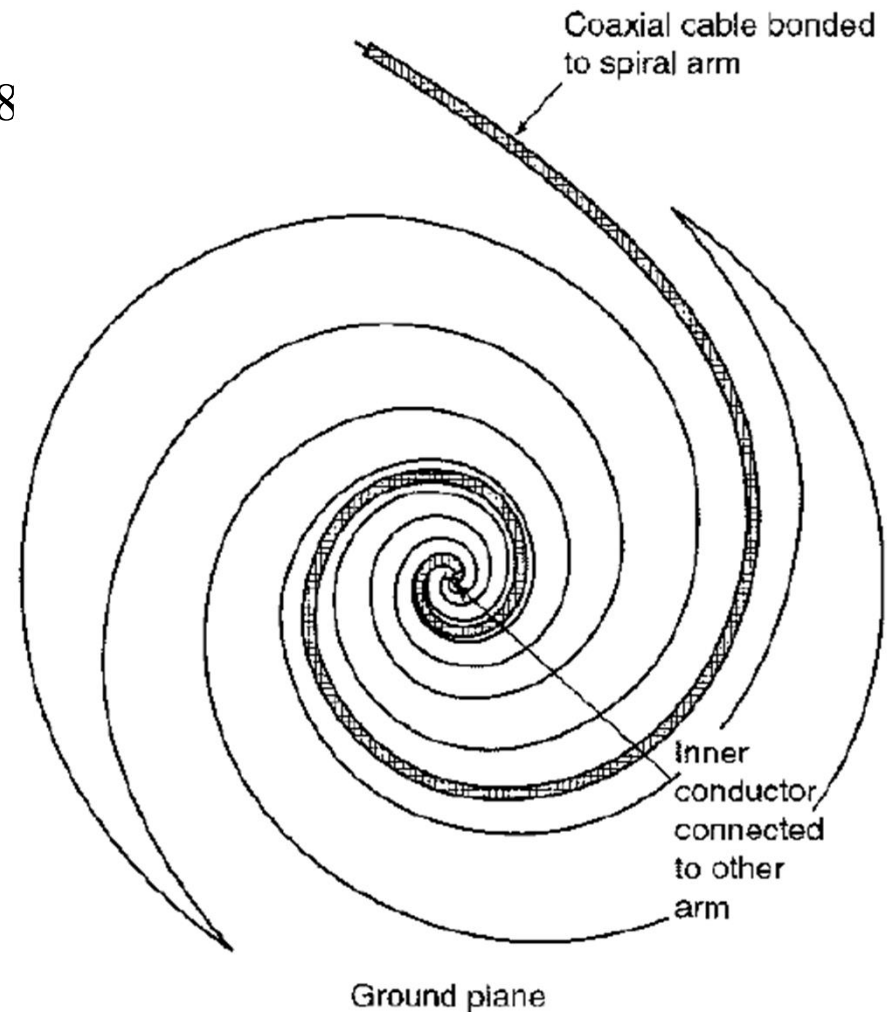
Fig. 6.22 Frequency-independent planar spiral antenna

In practice, it is more convenient to cut the slots for the antenna from a large ground plane, as done by Dyson, and feed the antenna with a coaxial cable bonded to one of the spiral arms as in Fig. 6.19 the spiral acting as a balun. A dummy cable may be bonded to the other arm for symmetry but is not shown.

Radiation for the antennas of Fig. 6.18 and 6.23 is bidirectional broadside to the plane of the spiral. The patterns in both directions have a single broad lobe so that the gain is only a few dBi. The input impedance depends on the parameters δ and a and the terminal separation.

Figure 6.23
Frequency-independent planar spiral antenna cut from large ground plane

Coaxial cable bonded to spiral arm

inner conductor connected to other arm

Ground plane

6.6.2 The Frequency-Independent conical-spiral antenna

A tapered helix is a conical-spiral antenna.

Fig. 6.24 Several frequency-independent conical spiral antennas

A typical balanced 2-arm Dyson conical spiral is shown in Fig. 6.25. The conical spiral retains the frequency-independent properties of the planar spiral while providing broad-lobed unidirectional circ ularly polarized radiation off the small end or apex of the cone. As with the planar spiral, the two arms of the conical spiral are fed at the centerpoint or apex from a coaxial cable boned to one of the arms, the spiral acting as a balun. For symmetry a dummy cable may be bonded to the other arm, as suggested in Fig. 6.25. In some models the metal straps are dispensed with and the cables alone used as the spiral conductors.
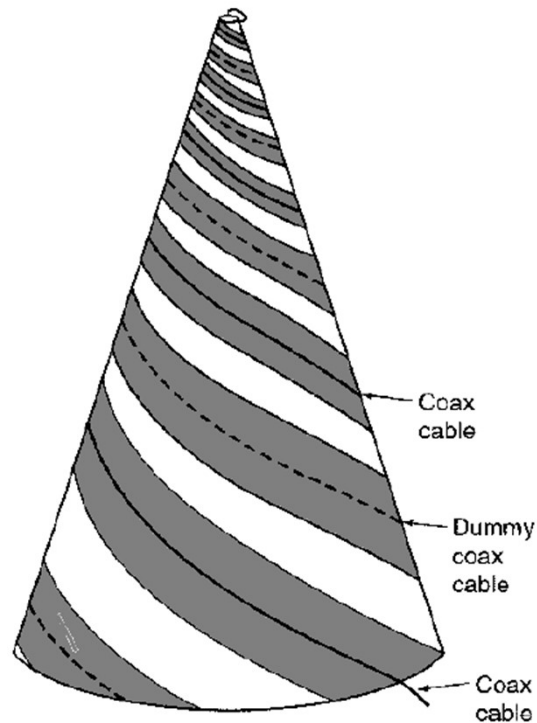

Fig. 6.25
Dyson 2-arm balanced conical-spiral (backward-fire) antenna. Polarization is RCP. Inner conductor of coax connects to dummy at apex.

According to Dyson, the input impedance is between 100 and 150 Ω for a pitch angle $\alpha = 17°$ and full cone angles of 20 to 60°. The smaller cone angles (30° or less) have higher front-to-back ratios of radiation. The bandwidth, as with the planar spiral, depends on the ratio of the base diameter ($\sim\lambda/2$ at the lowest frequency) to the truncated apex diameter ($\sim\lambda/4$ at the highest frequency). This ratio may be made arbitrarily large.
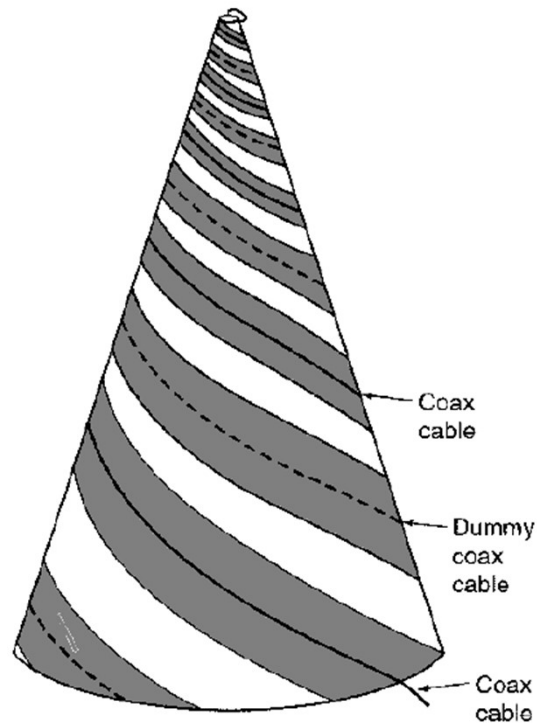

Coax cable

Dummy coax cable

Coax cable

Fig. 6.25
Dyson 2-arm balanced conical-spiral (backward-fire) antenna. Polarization is RCP. Inner conductor of coax connects to dummy at apex.
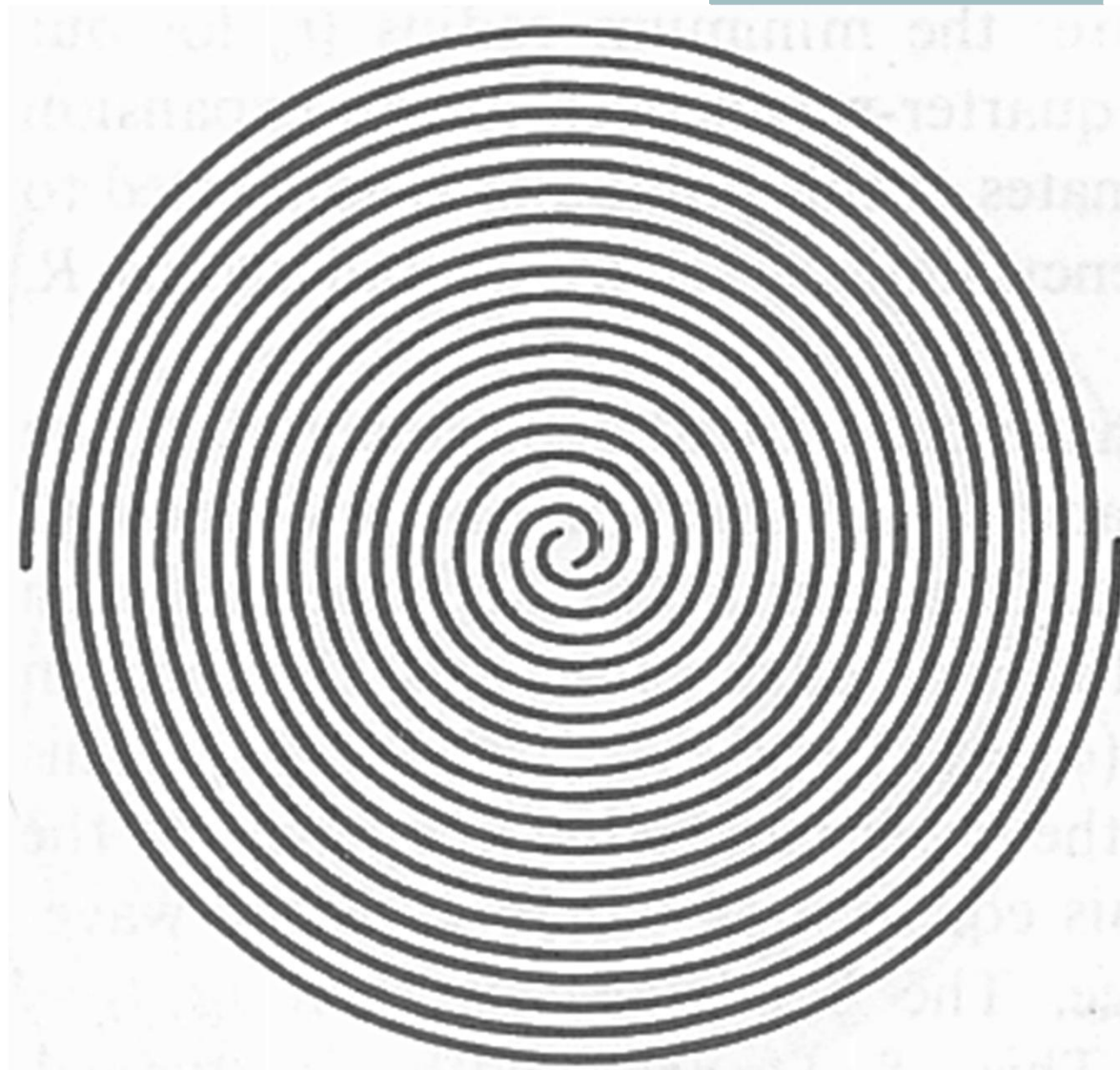
Fig. 6.26 The Archimedean spiral antenna

6.7 The Log-periodic Antenna

So called because the structure repeats periodically with the logarithm of the frequency. Put another way, the structure doubles for each doubling of the wavelength.

Fig. 6.27 Wideband log-periodic Antenna

The basic concept is that a gradually expanding periodic structure array radiates most effectively when the array elements (dipoles) are near resonance so that with change in frequency the active (radiating) region moves along the array.

The log-periodic dipole array is a popular design. Referring to Fig 6.28, the dipole lengths increase along the antenna so that the included angle α is a constant, and the lengths l and spacings s of adjacent elements are scaled so that

$$\frac{l_{n+1}}{l_n} = \frac{s_{n+1}}{s_n} = k \qquad\qquad (6.21)$$

Where k is a constant. At a wavelength near the middle of the operating range, radiation occurs primarily from the central region of the antenna, as suggested in Fig 6.28. The elements in this active region are about $\lambda/2$ long.
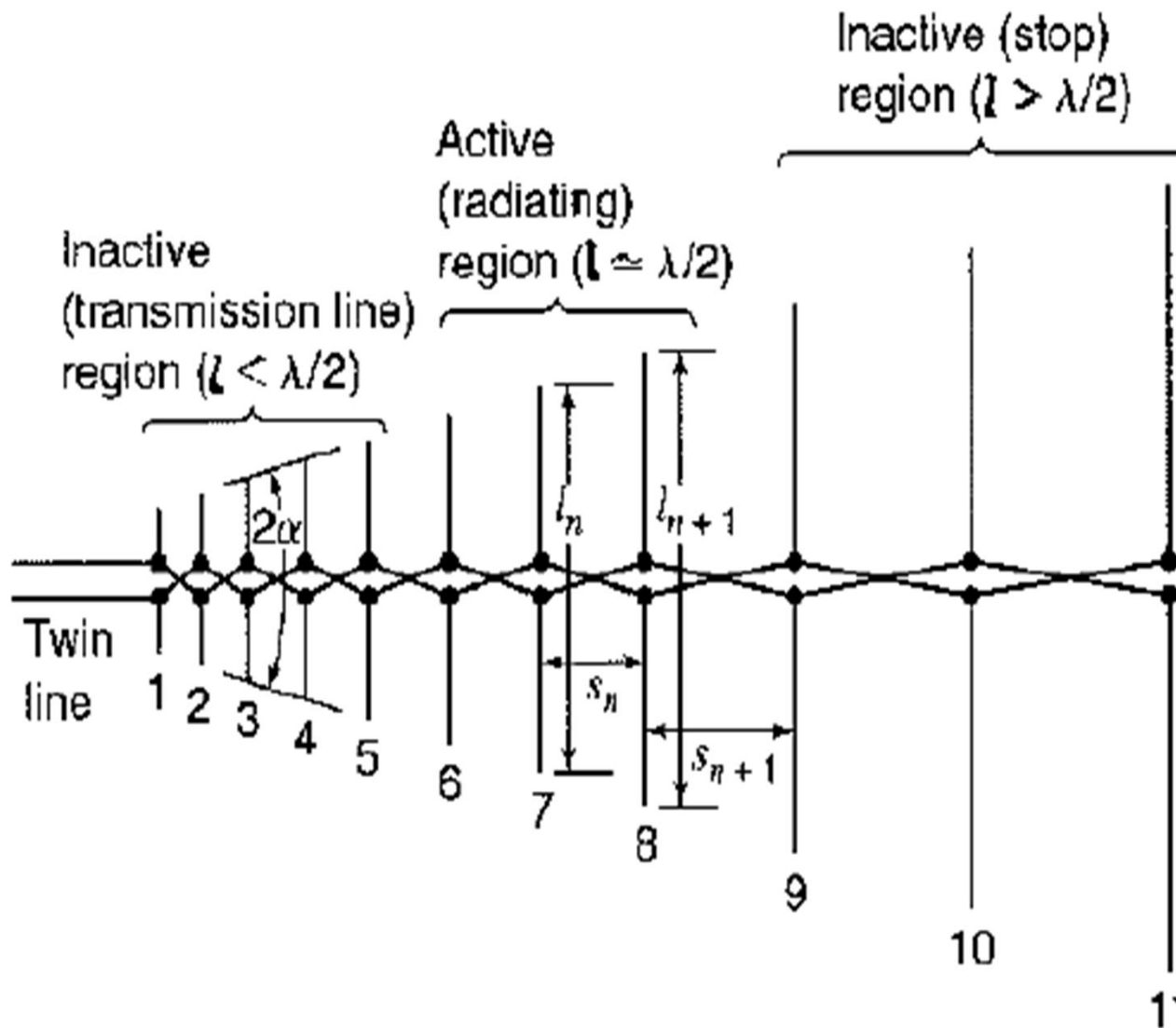
Log-periodic dipole array

Fig. 6.28
Isbell log-independent type of dipole array of 7dBi gain with 11 dipoles showing active central region and inactive regions (left and right ends).

Elements 9,10 and 11 are in the neighborhood of 1λ long and carry only small currents (they present a large inductive reactance to the line). The small current in elements 9, 10, 11 mean that the antenna is effectively truncated at the right of the active region. Any small fields from elements 9,10 and 11 also tend to cancel in both forward and backward directions. However, some radiation may occur broadside since the currents are approximately in phase. The elements at the left (1, 2, 3, etc.) are less than $\lambda/2$ long and present a large capacitive reactance to the line. Hence, currents in these elements are small and radiation is small.

Thus, at a wavelength λ , radiation occurs from the middle portion where the dipole elements are ~$\lambda/2$ long. When the wavelength is increased the radiation zone moves to the right and when the wavelength is decreased it moves to the left with maximum radiation toward the apex or feed point of the array.

At any given frequency only a fraction of the antenna is used (where the dipoles are about $\lambda/2$ long). At the short-wavelength limit of the bandwidth only 15 percent of the length may be used, while at the long-wavelength limit a larger fraction is used but still less than 50 percent.

$(l_{n+1} - l_n)/2$

S

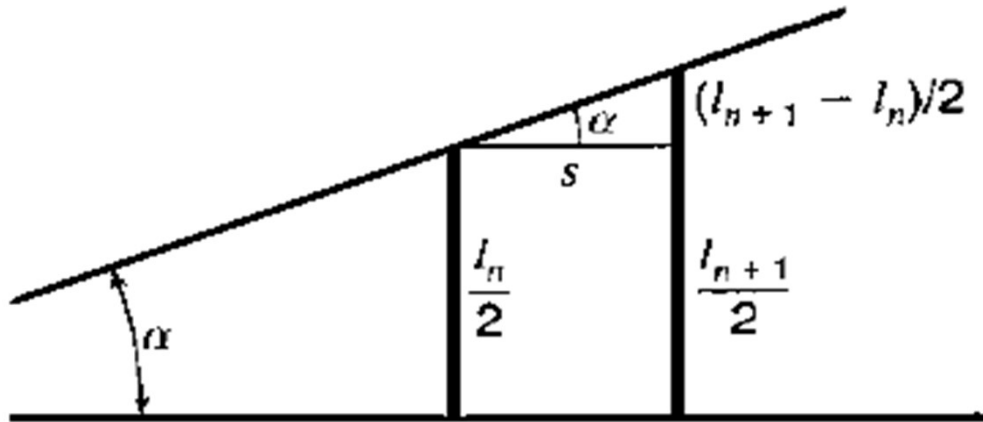$\dfrac{l_n}{2}$

$\dfrac{l_{n+1}}{2}$

Fig. 6.29
Log-periodic array geometry for
determining the relation of parameters.

From the geometry of Fig. 6.29 for a section of the array, we have

$$\tan\alpha = \frac{(l_{n+1} - l_n)/2}{S} \tag{6.22}$$

Or from (5.21),

$$\tan\alpha = \frac{[1 - (1/k)](l_{n+1}/2)}{S} \tag{6.23}$$

Taking $l_{n+1} = \lambda/2$ (when active) we have

$$\tan\alpha = \frac{1 - (1/k)}{4s_\lambda} \tag{6.24}$$

Where

$\alpha = apex\ angle$
$k = scale\ factor$
$s_\lambda = spacing\ in\ wavelength\ shortward\ of\ \lambda/2\ element$

Specifying any 2 of the 3 parameters $\alpha, k \ and \ s_\lambda$ determines the third. The relationship of the 3 parameters is displayed in Fig. 6.30 with the optimum design line (maximum gain for a given value of scale factor k) and gain along this line。

The length l (and spacing s) for any element $n + 1$ is k^n greater than for element 1, or

$$\frac{l_{n+1}}{l_1} = k^n = F \qquad\qquad (6.25)$$

Where $F = $ frequency ratio or bandwidth

Thus, if $k = 1.19 \ and \ n = 4, F = k^4 = 1.19^4 = 2$ and element $5(= n + 1)$ is twice the length l_1 of element 1. Thus, with 5 elements and $k = 1.19$, the frequency ratio is $2 \ to \ 1$.
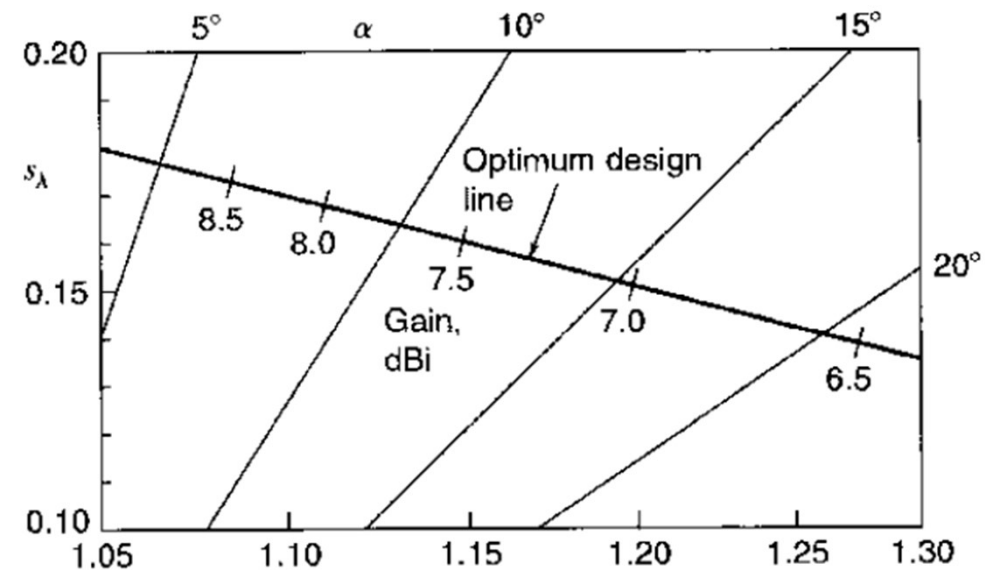
Fig. 6.30
Relation of log-periodic Array parameters of apex angle α, scale factor k and spacing s_λ with optimum design line and gain values.

EXAMPLE 6-1

Design a log-periodic dipole array with 7dBi gain and a 4 to 1 bandwidth. Specify apex angle α , scale constant k and number of elements.

■ Solution

From Fig. 6.24, the 7 dBi point on the maximum gain line corresponds to the apex angle $\alpha = 15°$ and k = 1.2. (We also note that $s_\lambda = 0.15$.) Form (7),

$$k^n = F \qquad or \qquad n \ln k = \ln F \qquad (6.26)$$

And

$$n = \frac{\ln F}{\ln k} = \frac{\ln 4}{\ln 1.2} = \frac{1.386}{0.182} = 7.6 \qquad (6.27)$$

Taking $n = 8, n + 1 = 9$. Adding 2 more elements for a conservative design brings the total to 11.

Details of construction and feeding are shown in Fig. 6.31 .The arrangement in (a) is fed with coaxial cable, the one at (b) with twin line.
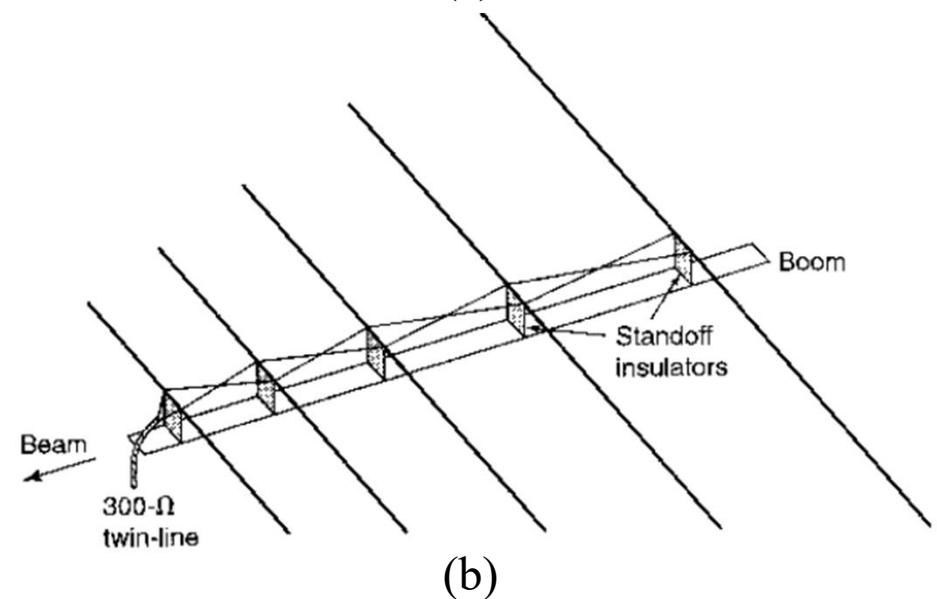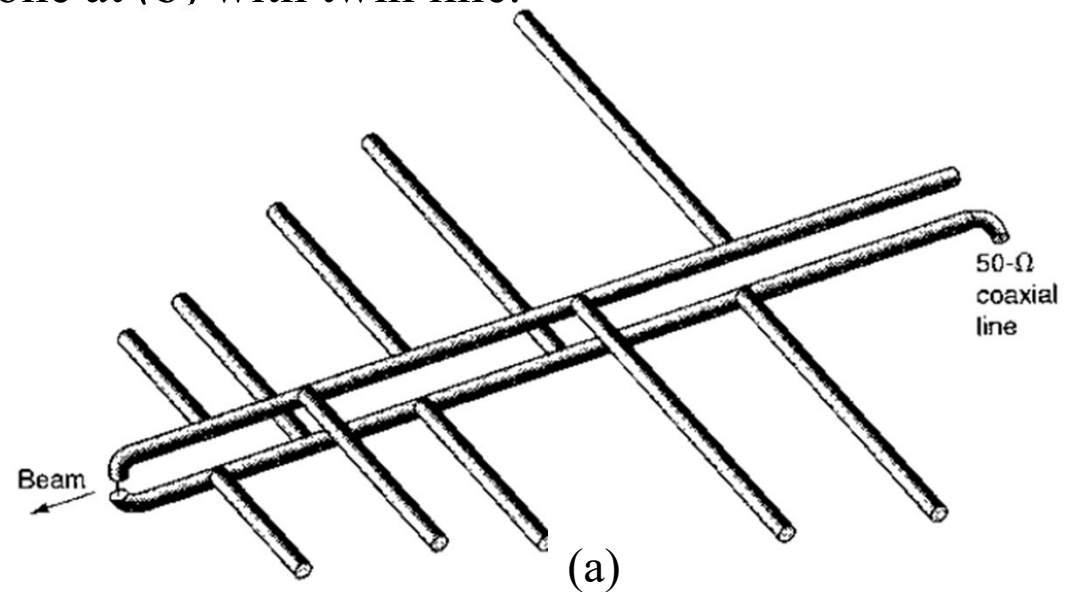

(a)

Fig. 6.31
Construction and feed details of log-periodic dipole array. Arrangement at (a) has a 50- or 70-Ω coaxial feed. The one at (b) has criss-crossed open-wire line for 300-Ω twin-line feed.

(b)

To obtain more gain than with a single log-periodic dipole array, 2 arrays may be stacked. However, for frequency-independent operation, Rumsey's principle requires that the locations of all elements be specified by angles rather than distances. This means that both log-periodic arrays must have a common apex, and, accordingly, the beams of the 2 arrays point in different directions.

For a stacking angle of $60°$, the situation is as suggested in Fig. 6.32 for dipole arrays of the type shown in Fig. 6.28 and 6.31. The array in Fig. 6.32 b is a skeleton-tooth or edge-fed trapezoidal type. Wires supported by a central boom replace the teeth of the antenna.

For very wide bandwidths the log-periodic array must be correspondingly long. To shorten the structure, Paul Mayes and Robert Carrel, of the University of Illinois, developed a more compact V-dipole array which can operate in several modes. In the lowest mode, with the central region dipoles $\sim \lambda/2$ long, operation is as already described. However, as the frequency is increased to the point where the shortest elements are too long to give $\lambda/2$ resonance, the longest elements become active at $3\lambda/2$ resonance. As the frequency is increased further, the active region moves to the small end in the $3\lambda/2$ mode.

With still further increase in frequency the large end becomes active in still higher-order modes. The forward tilt of the V-dipoles has little effect on the $\lambda/2$ mode but in the higher modes provides essential forward beaming. An example of a V-dipole array is shown in Fig. 6.32.
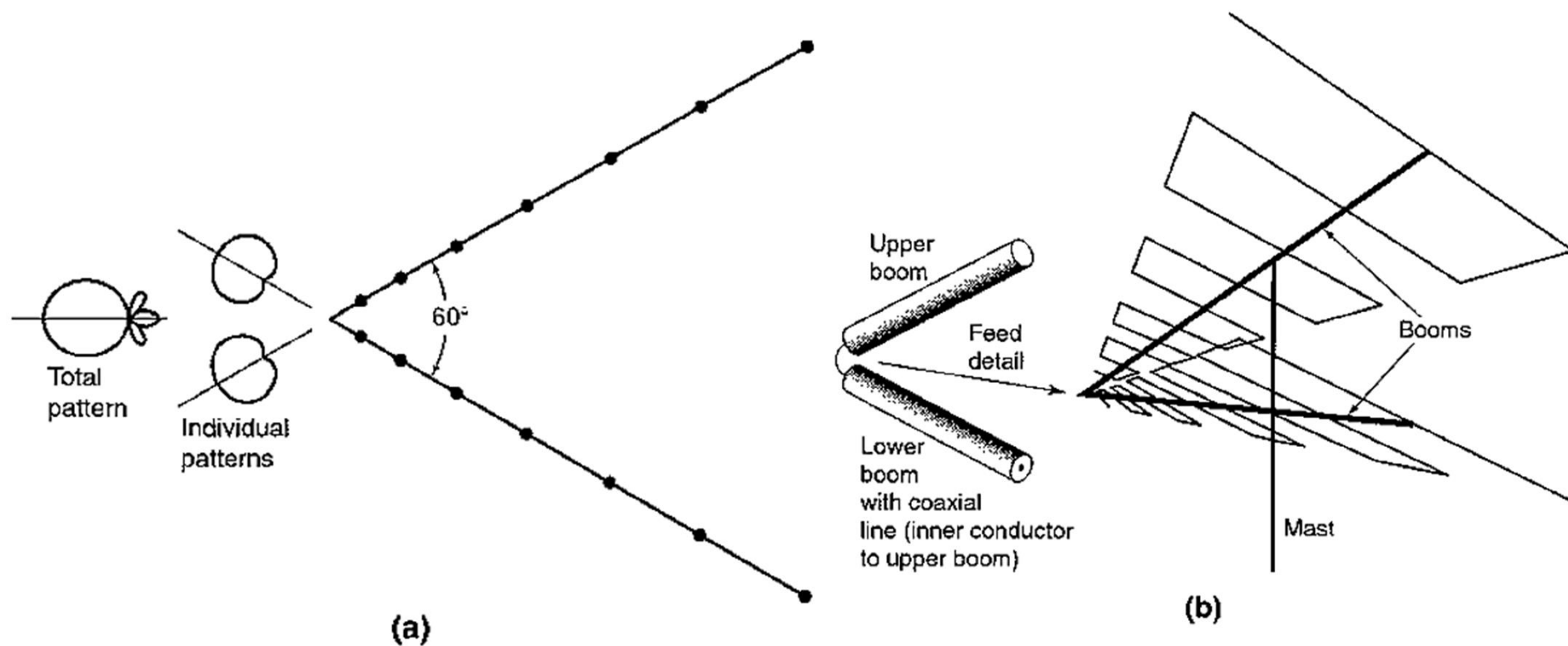
Fig. 6.32
Stacked log-periodic arrays, with dipole type, as in Figs 6.22 and 6.23 at (a) and trapezoidal or edge-fed type at (b).

6.7.2 The Composite Yagi-Uda-Corner-Log-Periodic(Yucolp) Array

For ultimate compactness and gain, to cover the 54 to 890 MHz U.S. TV and FM bands, a hybrid composite YUCOLP (Yagi-Uda-Corner-Log-Periodic) array is a popular design.

A typical model, shown in Fig. 6.33, has an $\alpha = 43°, k = 1.3$ LP array of 5V-dipoles to cover the 54 to 108 MHz TV and FM bands with a 6 dBi gain in the $\lambda/2$ mode, the 174 to 216 MHz band with 8 or 9 dBi gain in the $3\lambda/2$ mode and a square-corner-YU array to cover the 470 to 890 UHF TV band with a 7 to 10 dBi gain. The total included angle of the V-dipoles is 120°. The corner-YU array is similar in design to the one in Fig. 6.28.

As frequency increases, the active region moves from the large to the small end of the LP array in the $\lambda/2$ mode, then from the large to the small end in the $3\lambda/2$ mode, next to the corner reflector and finally to the YU array. The corner-YU array provides more gain for the UHF band than possible with a high-frequency extension of the LP array.
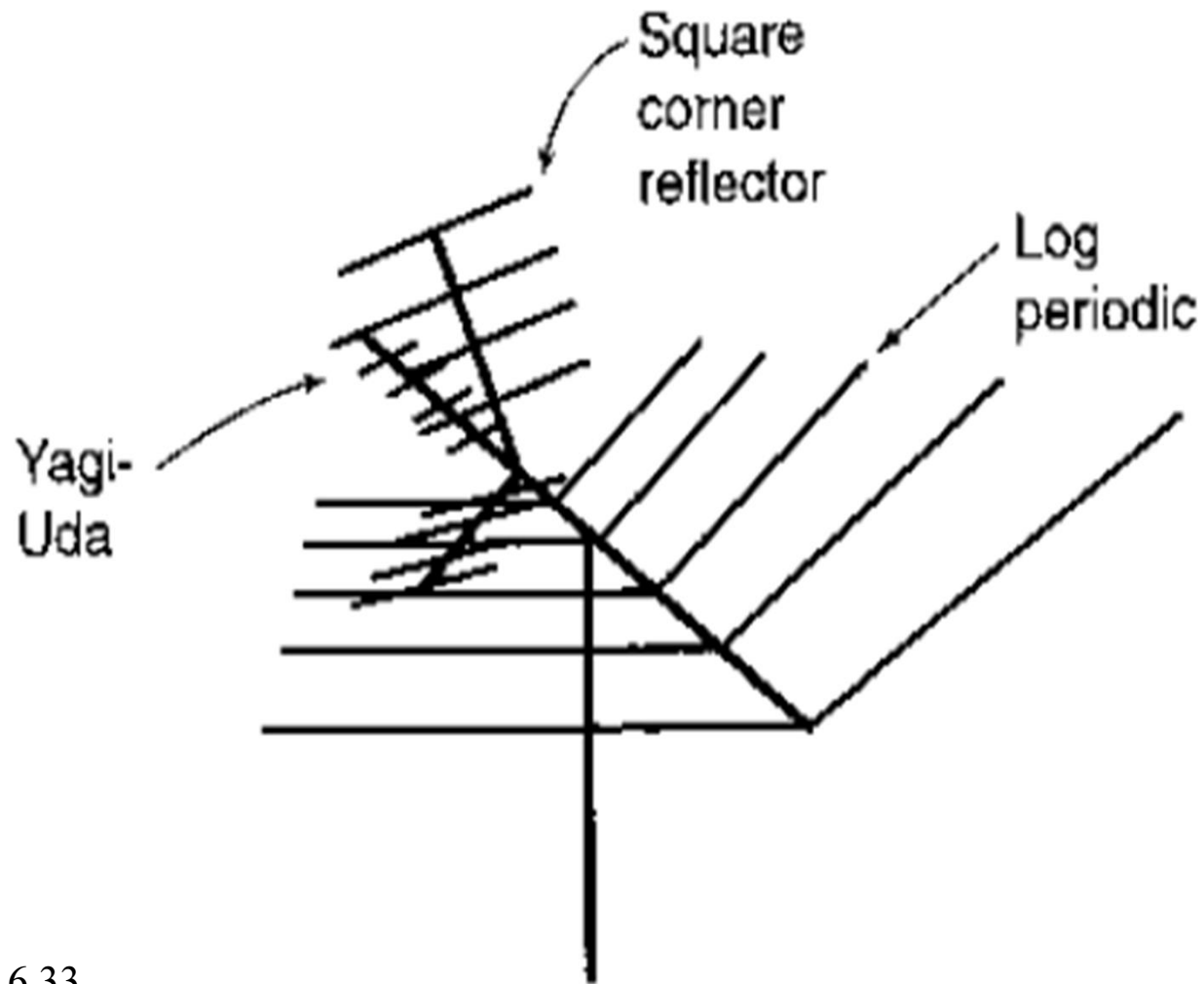
Fig. 6.33
YUCOLP (Yagi-Uda-Corner-Log-Preiodic) hybrid array for covering U.S. VHF TV and FM bands and UHF TV band. The YU-corner combination provides higher gain for the UHF TV band than an extension of the LP dipole array.